SCIENTIFIC REPORTS

OPEN

SUBJECT AREAS:
MAGNETIC DEVICES
MAGNETIC PROPERTIES AND MATERIALS
APPLIED PHYSICS
SPINTRONICS

Received
10 April 2013

Accepted
5 September 2013

Published
15 October 2013

Correspondence and requests for materials should be addressed to A.E. (a.erbe@hzdr.de)

Lateral spin transfer torque induced magnetic switching at room temperature demonstrated by x-ray microscopy

M. Buhl[1,2], A. Erbe[1], J. Grebing[1], S. Wintz[1,2], J. Raabe[3] & J. Fassbender[1,2]

[1]Helmholtz-Zentrum Dresden-Rossendorf, [2] Technische Universität Dresden, [3]Paul Scherrer Institut.

Changing and detecting the orientation of nanomagnetic structures, which can be used for durable information storage, needs to be developed towards true nanoscale dimensions for keeping up the miniaturization speed of modern nanoelectronic components. Therefore, new concepts for controlling the state of nanomagnets are currently in the focus of research in the field of nanoelectronics. Here, we demonstrate reproducible switching of a purely metallic nanopillar placed on a lead that conducts a spin-polarized current at room temperature. Spin diffusion across the metal-metal (Cu to CoFe) interface between the pillar and the lead causes spin accumulation in the pillar, which may then be used to set the magnetic orientation of the pillar. In our experiments, the detection of the magnetic state of the nanopillar is performed by direct imaging via scanning transmission x-ray microscopy (STXM).

The state of small magnetic entities has been used for data storage for some decades. Developments, *e.g.* based on giant magnetoresistance (GMR)[1,2] or tunnelmagnetoresistance (TMR)[3,4] effects, have enabled the nanoscale integration of these entities into large area devices such as hard disk drives. The state of these structures is usually set by the application of external magnetic fields. The generation of these fields at the location of the nanoscale magnetic memory requires the very precise positioning of a magnetic write head with respect to the element. This process, however, has not only the drawback of being time-consuming and technologically involved, but is also accompanied by parasitic stray fields that may limit the achievable storage density. Therefore, techniques allowing for magnetic switching without the necessity of applying an external field have been investigated extensively during the past years in the field of spintronics[5], a terminus which stands for the concept of using the electron spin for information storage and manipulation. The torque which is exerted by a spin polarized current on the electrons in a conductor depends on the relative orientation of the corresponding spin moments. A spin polarized current entering a ferromagnetic element thus may change the magnetization orientation of this element and by this information can be stored inside it. The underlying effect, called spin transfer torque (STT)[6,7], has been studied intensively in several magnetization switching experiments using time-resolved STXM[8–10]. However, most of the structures investigated so far have in common that they require vertical integration of the memory cell in the so-called current perpendicular to the plane (CPP) configuration, making the circuit design and fabrication rather complicated. In contrast, demonstration of STT induced switching of magnetic nanostructures with a purely horizontal contact layout would open various efficient possibilities for large scale integration of STT magnetic memories. In our layout, the number of necessary lithography steps is reduced to 2 as opposed to at least 3 steps in the case of vertical magnetic nanostructures. In addition, the technologically challenging side-wall isolation of the magnetic pillars is not necessary in our design.

We have developed a layout consisting of a nanoscale, elliptic magnetic structure ("nanopillar") and two micronscaled, rectangular magnetic elements ("polarizers") as shown in figure 1. Both, the central pillar and the surrounding polarizers are fabricated from CoFe at a thickness of 8 nm. The magnetic anisotropy at this thickness enforces the magnetization to be oriented in the plane of the film. In addition, the elliptical shape of the central pillar leads to anisotropy energy in the plane of the pillar, which is minimized for a magnetization along the long axis of the ellipse. Thus, two energetically equivalent magnetic configurations arise as ground states for the pillar.

The electrical connection between the polarizers and the pillar is provided by a Cu line of 5 nm thickness and 100 nm width that also extends to underneath the polarizers. The total length of the Cu line between the polarizers is 280 nm, which is of the order of the typical spin coherence length in pure Cu at room temperature[11]. Our circuit thus allows us to generate a spin-polarized current below one of the polarizers, which flows

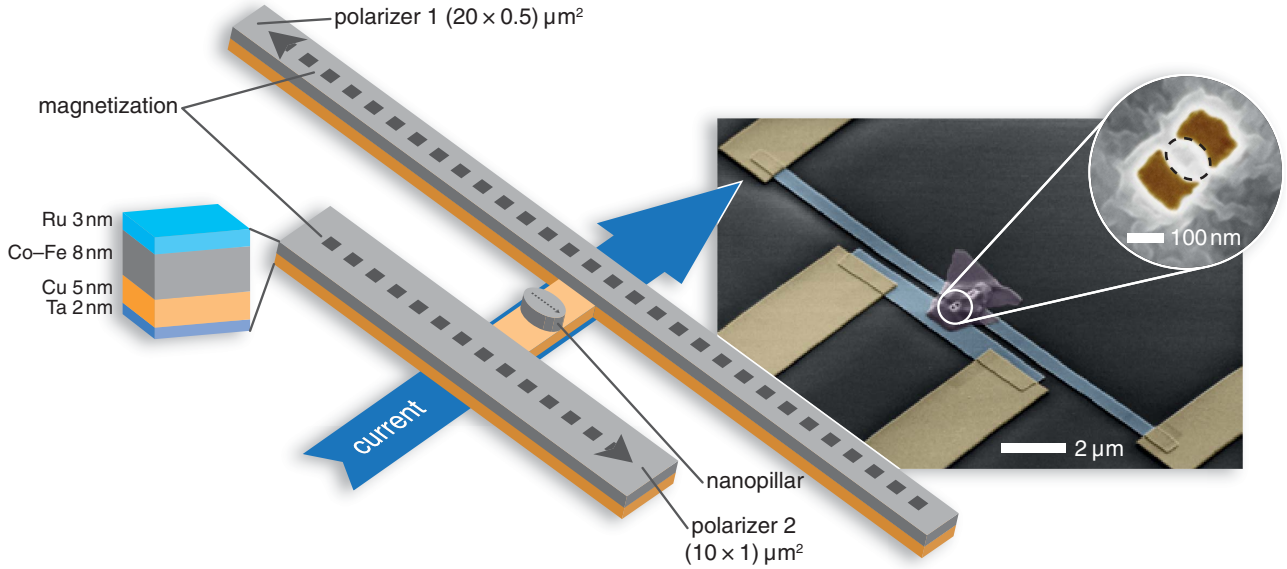

Figure 1 | Schematic layout of the current in plane spin transfer torque (STT CIP) structure (left) and scanning electron microscopy (SEM) images (right). The magnetic pillar (marked by dashed lines in the zoom shown upper right) is placed in between two polarizers with aspect ratios 10 µm × 1 µm and 20 µm × 0.5 µm, respectively. Due to the different aspect ratios the magnetizations of the polarizers can be set antiparallel, as sketched by the dotted arrows. A Cu line is used to carry a spin polarized under the polarizers and the pillar. Depending on its polarization, this current switches the pillar between the two magnetization directions, which are energetically favored due to the elliptic shape of the pillar (left and right in the zoom shown in the center).

underneath the pillar into the direction of the second polarizer. This kind of design is called a current in plane (CIP) configuration. Theoretical calculations have shown that in such CIP configuration the efficiency for STT induced magnetization switching due to spin diffusion is of similar order as in CPP configurations, i.e. configurations in which the charge current passes directly through the pillar[12]. Recent experiments have indeed demonstrated electrical measurements for the switching of magnetic nanostructures in CIP configurations[13] at low temperatures (between 10 K and 77 K). Here, we show the first experimental realization of directly imaging the magnetic state of a nanostructure in CIP configuration before and after switching events by using STXM[14] and exploiting x-ray magnetic circular dichroism (XMCD) effects. Corresponding micrographs and the construction of the magnetic contrast images are demonstrated in figure 2. Furthermore, the size scale and the layout of our sample even allow for the operation and detection of CIP STT switching at room temperature. This opens the way for a fundamental characterization of the switching mechanisms in static and dynamic experiments as well as for the development of possible applications incorporating CIP configurations in this area.

Results

The magnetization of the pillar can be reversed by current pulses passing underneath the polarizers leading to configurations with the magnetization pointing in either of the two directions of the long axis ("left" or "right" in the following discussion). The initial magnetization orientation of the pillar depends on the externally applied magnetic field and the stray fields originating from the polarizers. Using an external magnet, fields in the range of -30 mT $< \mu_0 H_{ext} <$ 30 mT are generated at the location of the sample. By applying such fields, configurations with a bistable pillar magnetization and two oppositely magnetized polarizers can be obtained, as shown in figure 2. This is the main prerequisite for an experimental condition where switching between the two magnetization orientations of the pillar is possible by spin transfer torque *only*.

In this configuration a current pulse, which has become spin-polarized beneath the initial polarizer, passes underneath the pillar. The magnetization of the pillar is imaged before and after the pulse. Figure 3 illustrates the reproducible switching of the pillar's magnetization state from left (dark contrast) to right (bright contrast) and back without external field.

This switching process was repeated several times in a single structure and was also measured in various samples produced on different chips, in order to show the reproducibility of our results. The details of the switching process (e.g. necessary current density) vary for the individual nanostructures, but the general switching behavior proved to be reliable and reproducible. In total, we have successfully demonstrated switching with and without supporting field in five different samples produced in two different production runs. The details of the switching events are summarized in the supplementary information (SI).

Discussion

In order to prove the significance of the STT effect for the switching processes observed we will discuss and subsequently exclude other possible switching mechanisms, such as induced by stray fields, Oerstedt fields, or device heating, in the following.

In order to confirm that the magnetic field in the center of our structure is indeed zero, micromagnetic simulations of the stray field originating from the polarizers in the configuration shown in figure 3 were carried out (details of the simulation can be found in the SI). As expected, the polarizer induced stray fields at the location of the pillar are negligible ($\mu_0 H < 0.1$ mT). We have further tested the influence of magnetic fields on the magnetization of the pillar by performing measurements at externally applied, supporting fields H_{ext} (shown in the SI). The values of the current density needed to perform switching, j_{sw} in the nanopillars are similar for all elements, regardless of the value of H_{ext}. We can thus conclude that application of H_{ext} does not alter the switching for the majority of the structures. It is, however, remarkable that a small number of samples can be switched with applied H_{ext}, only. This supporting field then needs to be close to the switching field without additional spin transfer torque. In most cases, however, the values of j_{sw} are symmetric around 0 T. This indicates that the influence of stray fields originating from the polarizers is

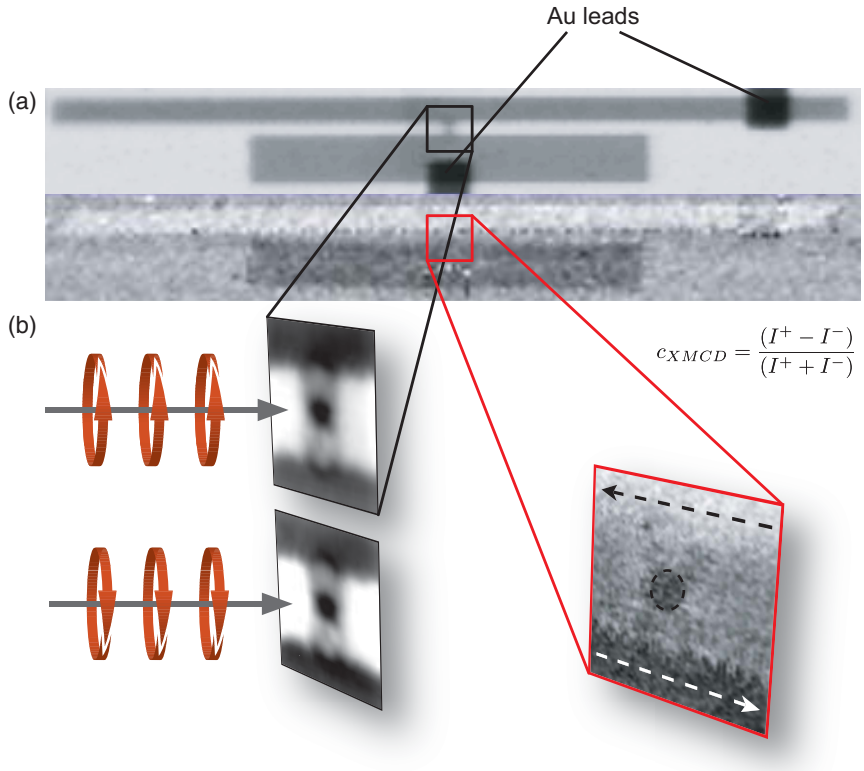

Figure 2 | (a) STXM image of the central area of the spin torque device including the two polarizers and the magnetic pillar in the center. The upper image shows the direct absorption contrast caused by the metallic layers. The images are recorded at the absorption maximum of Co, *i.e.* $E = 780$ eV. The lower image shows the contrast given by different absorption of the transmitted x-rays due to XMCD indicating the magnetization directions of the two polarizers. In our images black structures correspond to the magnetization pointing to the right side (positive values of H), and white structures to the magnetization pointing to the left side (negative H). This contrast is achieved by depicting the normalized intensity difference $c_{\mathrm{XMCD}} = \frac{I^+ - I^-}{I^+ + I^-}$ of the two images taken at different polarizations. (b) Zoom on the central pillar and construction of the magnetic contrast images. The central region containing the nanopillar (highlighted by the dashed circle) is scanned with circularly polarized x-rays. The contrast of spin-polarized regions depends on the polarization, thus subtraction of the images shows the magnetic contrast in the structure. It can be seen in (a) that the Au leads connecting the polarizers to the current pulser disappear in the magnetic contrast image.

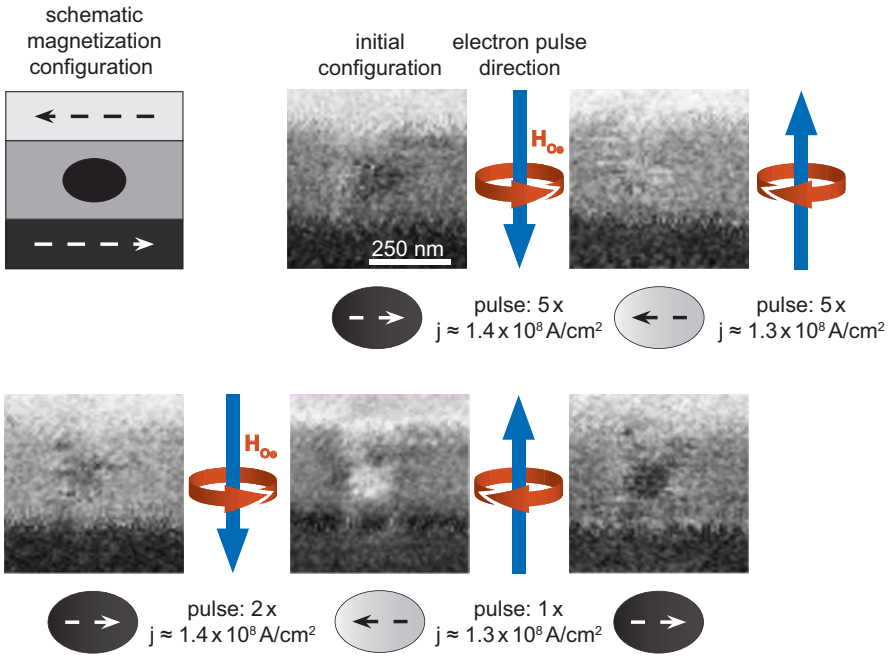

Figure 3 | **Switching of the pillar without supporting magnetic field.** It is shown that switching in both directions can be performed at identical absolute values of the current density using 5 and 2 consecutive pulses, as well as single pulses.

negligible in our geometry. As already mentioned, this statement is supported by micromagnetic simulations shown in the SI. A parallel arrangement of the magnetization of the polarizers leads to increased stray fields in the gap between the polarizers. We can induce switching in this configuration, as well, opposite to the direction favored by the stray fields, giving an additional hint for the fact that stray fields play a negligible role in our experiments.

An electrical current flowing through a nanowire is accompanied by a magnetic field, the so-called Oersted field indicated by the red arrows in figure 3. The direction and amplitude of this field for a wire of approximately 100 nm in diameter carrying a current of 4 mA can be estimated to be of the order $\mu_0 H \approx 8$ mT pointing in the plane of the pillar[15]. This field is of the order, but still below, the critical field needed for reversing the magnetization of the pillar. The direction of the Oersted field is pointing in the opposite direction of the spin torque in all switching events summarized in figure 3 and in the SI. We also performed experiments in which current pulses polarized in the initial magnetization direction of the pillar but with an Oersted field in the opposite direction were applied. In none of these experiments switching could be observed for the material composition discussed in this paper.

In order to estimate the thermal contribution to the magnetic switching of the pillar we need to estimate its magnetic energy. For an elliptical pillar with axes a and b we can calculate the demagnetization energies along the axes E_a and E_b, assuming a uniform magnetization along these axes[16]. For our geometry and a saturation magnetization $M_s = 1.9$ T/μ_0 we obtain a planar shape anisotropy energy $E_a - E_b = 2.5 \times 10^{-18}$ J. This energy is much larger than the thermal energy at temperatures, which are observed during the switching event (600 K, $k_B T = 8.2 \times 10^{-21}$ J). Therefore we can conclude that the nanopillars in the experiments are thermally stable even if the currents driven through the Cu wire lead to heating of the entire structure. In order to estimate the amount of heating, we have measured the resistance variation for an applied dc-current. As discussed in detail in the SI we can provide an upper boundary for the temperature of the wire $T_{wire} < 600$ K. This value is far below the Curie temperature of the bulk Co (T_{Curie}(Co) = 1400 K), as well. The superparamagnetic limit for Co nanostructures, which exceed volumes of 1×10^{-15} m^3, lies above 1000 K, therefore bulk values for Curie temperature are relevant here. As even for elevated temperatures the ratio of thermal and anisotropy energy is $\ll 1$, thermal effects can be neglected as mechanism significantly supporting the magnetization switching in our case.

We now turn to the discussion, whether our results can be explained by pure spin transfer torque switching. The geometry shown in figure 1 is optimized for the experiments performed using STXM. Therefore, no electrical transport measurements through the nanopillar can be performed in order to obtain values for the spin diffusion length in the Cu stripe or the degree of spin polarization of the conduction electrons of the CoFe elements. Without experimental values for these quantities, an estimate of the spin current passing underneath the pillar during each current pulse cannot be achieved. We therefore have to limit our discussion to a qualitative comparison between our structure and the structure reported by Yang *et al.*[13]. In both structures, a Cu line connects two magnetic structures, one of which is used as a polarizer, the other one as a detector for the spin polarized current. Our data are recorded on pillars consisting of CoFe, while the nanostructures in[13] are made from permalloy. The distance between the pillar and the polarizer is 90 nm in our structures as opposed to 270 nm reported in[13] or 400 nm in[17]. This explains, why we are able to observe spin transfer torque in our structures at room temperature in a CIP configuration.

We have shown that elliptical nanopillars can be switched between their two preferred magnetic states by passing a spin-polarized current underneath the pillars, and we can image the different states before and after the switching using STXM. For our structures (elliptical pillars with dimensions of 100 nm × 120 nm) we can exclude all other switching sources as, for example stray fields, Oersted fields or heating. This study, therefore, provides an unambiguous demonstration of the switching by spin transfer torque (STT) in a current in plane (CIP) geometry and paves the way for future developments of such structures aiming at integration of these structures into fully planar device architectures. Furthermore, time-resolved studies of the dynamics of this switching mechanism will be possible in the future.

Methods

The devices were fabricated on Si_3N_4membranes with a thickness of 100 nm. The metallic multilayers were deposited by magnetron sputtering before patterning the nanostructures in order to ensure optimal layer quality and interface integrity. The layers consist of 2 nm Ta for adhesion, 5 nm Cu for the conduction of the spin-polarized electrons, 8 nm of $Co_{80}Fe_{20}$, and a Ru capping layer of 3 nm. By varying the Fe content of the CoFe layer we can adjust the magnetic softness of the pillar[18] and, thus, the coercive field needed to switch the magnetization. Addition of Fe to the stack reduces, however, the imaging contrast of our structure in the STXM experiments (see below).

The metallized membranes were subsequently structured using electron beam lithography and dry etching using both positive and negative lithography steps. The metallic layers are removed using argon ion beam etching. In a first step, the polarizers and their connection including the pillar are defined by removing the stack at all other areas of the sample. The following lithography step removes the CoFe layer on top of the Cu leaving Cu leads between the polarizers and the pillar in the center of the structure. The areas with uncovered Cu would oxidize when exposed to air and are, therefore, covered with SiO_2 *in situ*. A scanning electron micrograph of the sample after these fabrication steps is shown in figure 1. The final processing step provides electrical contacts to the polarizers. These contacts are made of Au and are fabricated in a lift-off process. The samples are contacted on a circuit board with high-frequency source-drain connections.

The switching of the magnetic state of the nanopillar is performed by driving a pulse of spin-polarized current underneath and through the pillar. In order to generate this current pulse we apply a voltage pulse across the structure, leading to a current passing the polarizers and the Cu connection under the pillar. Depending on the resistance ratio between the Cu connection and the CoFe pillar, a fraction of the current flows through the pillar directly, as well. For the geometry and material composition in our experiment, we estimate that a fraction of 1/5 flows through the pillar leading to additional spin accumulation in the pillar. The different aspect ratios of the polarizers (shown in figure 1) lead to different coercive fields[19]; the magnetization points along the long axis of the polarizers and parallel to the surface of the sample. As a consequence the polarizers can be set in either one of the two available states with magnetization pointing to the left or to the right (see figure 1 for details) and in an antiparallel configuration, as well. The magnetization of the polarizers defines the majority charge carriers injected into the Cu lead connecting the two polarizers. Therefore we have the possibility to pass a spin-polarized current through the Cu connector, which is polarized in either one of the two directions, left or right. When the magnetization of the pillar at the center of the structure is antiparallel to the polarization of the current, spin transfer torque (STT)[20] acts on the spins in the pillar because of spin diffusion through the Cu/CoFe interface. The goal of our experiments is twofold: to demonstrate that STT is strong enough to switch the direction of magnetization of the pillar at nondestructive current levels, and to image the magnetic state of the pillar before and after switching.

In order to characterize the magnetic state of our structures, we perform magnetic imaging in a scanning transmission x-ray microscope (STXM) at the swiss light source (SLS) beamline X07DA (Pollux). Using circularly polarized x-rays we image the spin density of the unoccupied d-band exploiting the effect of x-ray magnetic circular dichroism (XMCD)[21] effect. The x-rays are focused by passing through a zone-plate with minimal structure sizes of 15 nm. This setup allows a resolution of structure sizes down to about 30 nm in the images for normal experimental conditions. Typical dimensions of the magnetic pillars in our experiments are 100 nm × 120 nm. We can, therefore, image the magnetization of individual pillars with high quality. The samples are mounted on the scanning stage of the beamline together with a metal-cored coil providing a static magnetic field parallel to the magnetization direction of the polarizers. This external field is used to define the magnetization of the polarizers and, in some of the experiments, as a supporting field aiding the switching of the pillar.

We perform measurements of the magnetic behavior of the pillar and the polarizers by changing the static magnetic field H_{ext} step by step and recording STXM images at each value of H_{ext}. A STXM overview of the whole configuration in antiparallel alignment can be seen in figure 2. Here, the magnetization of the pillar in the center always points parallel to one and anti-parallel to the other of the two polarizers. Thus, passing a current underneath the device in one direction can switch the magnetization of the pillar. Driving the current in the opposite direction provides spin polarization in the direction of the magnetization of the pillar at the interface and, therefore, does not lead to changes in the magnetization. Switching without a supporting magnetic field can be performed in both directions by varying the direction of the current as long as the magnetization directions of the polarizers do not change.

We would like to thank Alina Deac, Jürgen Lindner, Sibylle Gemming, and Kay Potzger for fruitful discussions, Kerstin Bernert, Gabi Steinbach, Julia Osten, and Tom Henschel for help during the experiments, and Patrick Matthes and Manfred Albrecht for sample preparation. This work was in part supported by BMBF.

1. Binasch, G., Grunberg, P., Saurenbach, F. & Zinn, W. Enhanced Magnetoresistance in Layered Magnetic-Structures with Antiferromagnetic Interlayer Exchange. *Phys. Rev. B* **39**, 4828 (1989).
2. Baibich, M. N. *et al*. Giant Magnetoresistance of (001)Fe/(001) Cr Magnetic Superlattices. *Phys. Rev. Lett.* **61**, 2472 (1988).
3. Moodera, J. S., Kinder, L. R., Wong, T. M. & Meservey, R. Large Magnetoresistance at Room-Temperature in Ferromagnetic Thin-Film Tunnel-Junctions. *Phys. Rev. Lett.* **74**, 3273 (1995).
4. Julliere, M. Tunneling Between Ferromagnetic-Films. *Phys. Lett. A* **54**, 225 (1975).
5. Sinova, J. & Zutic, I. New moves of the spintronics tango. *Nature Mat.* **11**, 368 (2012).
6. Slonczewski, J. C. Current-driven excitation of magnetic multilayers. *J. Magn. Magn. Mater.* **159**, L1 (1996).
7. Berger, L. Emission of spin waves by a magnetic multilayer traversed by a current. *Phys. Rev. B* **54**, 9353 (1996).
8. Acremann, Y. *et al*. Time-Resolved Imaging of Spin Transfer Switching: Beyond the Macrospin Concept. *Phys. Rev. Lett.* **96**, 217202 (2006).
9. Strachan, J. *et al*. Direct Observation of Spin-Torque Driven Magnetization Reversal through Nonuniform Modes. *Phys. Rev. Lett.* **100**, 247201 (2008).
10. Bernstein, D. *et al*. Nonuniform switching of the perpendicular magnetization in a spin-torque-driven magnetic nanopillar. *Phys. Rev. B* **83**, 180410 (2011).
11. Ji, Y., Hoffmann, A., Pearson, J. E. & Bader, S. B. Enhanced spin injection polarization in Co/Cu/Co nonlocal lateral spin valves. *Appl. Phys. Lett.* **88**, 1 (2006).
12. Wessely, O., Umerski, A. & Mathon, J. Theory of spin-transfer torque in the current-in-plane geometries. *Phys. Rev. B* **80**, 014419 (2009).
13. Yang, T., Kimura, T. & Otani, Y. Giant spin-accumulation signal and pure spin-current-induced reversible magnetization switching. *Nature Phys.* **4**, 851 (2008).
14. Raabe, J. *et al*. PolLux: A new facility for soft x-ray spectromicroscopy at the Swiss Light Source. *Rev. sci. instr.* **79**, 113704 (2008).
15. Moon, K. W., Lee, J. C., Rhie, K., Shin, K. H. & Choe, S. B. Detection of Local Oersted Field Generated at the Junction Between Ferromagnetic Nanowire and Electrode. *IEEE Trans. Magn.* **47**, 2508 (2011).
16. Beleggia, M., De Graef, M., Millev, Y. T., Goode, D. A. & Rowlands, G. Demagnetization factors for elliptic cylinders. *J. Phys. D-Appl. Phys.* **38**, 3333 (2005).
17. Kimura, T., Otani, Y. & Hamrle, J. Switching magnetization of a nanoscale ferromagnetic particle using nonlocal spin injection. *Phys. Rev. Lett.* **96**, 037201 (2005).
18. Wang, S. X., Sun, N. X., Yamaguchi, M. & Yabukami, S. Sandwich films - Properties of a new soft magnetic material. *Nature* **407**, 150 (2000).
19. Meiklejohn, W. H. & Bean, C. P. New magnetic anisotropy. *Phys. Rev.* **105**, 904 (1957).
20. Zutic, I., Fabian, J. & Sarma, S. Spintronics: Fundamentals and applications. *Rev. Mod. Phys.* **76**, 323 (2004).
21. Schutz, G. *et al*. Absorption of circularly polarized x-rays in iron. *Phys. Rev. Lett.* **58**, 737 (1987).

Author contributions

M.B. and J.G. carried out the device fabrication. M.B., A.E., J.G., S.W. and J.R. performed the STXM experiments. A.E., M.B., S.W. and J.G. interpreted the data. J.F. and A.E. designed the experiment, M.B. and J.G. prepared the figures. All authors discussed the results and contributed to the manuscript preparation.

Additional information

Supplementary information accompanies this paper at http://www.nature.com/scientificreports

Competing financial interests: The authors declare no competing financial interests.

How to cite this article: Buhl, M. *et al*. Lateral spin transfer torque induced magnetic switching at room temperature demonstrated by x-ray microscopy. *Sci. Rep.* **3**, 2945; DOI:10.1038/srep02945 (2013).